# The Cosmic-Ray Extensive Air Shower Environment of Thunderstorms

N. C. Lindy[1], E. R. Benton[1*], A. N. Ruse[1], D. Petersen[2], and W. Beasley[2]

[1]Radiation Physics Laboratory, Oklahoma State University
[2]School of Meteorology, University of Oklahoma

**Abstract:** According to the Relativistic Runaway Electron Avalanche (RREA) model, a population of seed electrons from cosmic ray extensive air showers (CREAS) is required to initiate a lightning discharge. Using the CREAS Monte Carlo code CORSIKA 6.790, we have determined the energy spectrum and ambient flux of secondary electrons in both fair weather and thunderstorm atmospheric conditions <12 km above sea level. The secondary electron energy spectrum contains a population of >100 MeV electrons, which are able to generate many additional relativistic secondary electrons and possibly generate high energy (>1 MeV) bremsstrahlung photons. The ambient flux of secondary electrons increases exponentially with altitude with a value of 260 electrons $m^{-2}$ $sr^{-1}$ $s^{-1}$ at 8 km, but the electron flux can be $>10^5$ $m^{-2}$ inside the core of a $10^{16}$ eV CREAS. High energy secondary electrons within the core of a CREAS may be a large enough population of seed electrons to initiate a lightning discharge.

## INTRODUCTION

The Relativistic Runaway Electron Avalanche (RREA) model proposed by Gurevich et al. [1992] is currently considered one of the most likely explanations for lightning initiation within thunderstorms [McCarthy and Parks 1992; Dwyer et al. 2003; Dorman 2004]. The RREA model theorizes that a population of high energy electrons traveling through the strong electric fields of a thunderstorm will generate enough secondary electrons to initiate an electrical breakdown in the atmosphere [Gurevich et al. 1992; Gurevich et al. 2004; Milikh and Roussel-Dupre 2010].

High energy electrons are generated in cosmic ray extensive air showers (CREAS). CREASs are initiated by energetic cosmic ray protons and heavy ions that enter and undergo nuclear interactions within the Earth's atmosphere. Protons dominate the cosmic ray flux at the top of the atmosphere, which is parameterized by Horandel [2003],

$$\varphi_{primary}\ E_p \ = \ 8.73 * 10^{-2}\ m^{-2} sr^{-1} s^{-1} \quad \frac{E_p}{10^{12} eV}^{-2.71}, \qquad (1)$$

where $\varphi_{primary}$ is the cosmic ray primary flux at the top of the atmosphere and $E_p$ is the primary proton energy. The greater the energy of the primary particle that initiates the CREAS, the larger the number of secondary particles, including high energy electrons, that are produced in the CREAS [Grieder 2010]. According to equation (1), the primary proton flux decreases with cosmic ray primary energy, so the atmosphere has many more low energy CREAS traveling than the larger high energy CREAS. This causes ambient secondary electron environment to be dominated by the frequent smaller low energy (~ $10^{10}$ eV primary) CREASs and not the large, higher energy (>$10^{15}$ eV primary) CREASs.

* Corresponding Author: Dr. Eric Benton, Radiation Physics Laboratory, Oklahoma State University, 1110 Innovation Way Dr. #100, Stillwater, OK, USA, Email: eric.benton@okstate.edu

High energy electrons are created in the dense shower core of the CREAS. The shower core is the region immediately surrounding the shower axis, i.e. the path of the CREAS primary. The shower core is made up of very high energy (>100 MeV) secondary particles that due to their high momentum travel in the original direction of the CREAS primary. These high energy particles are responsible for generating high energy secondary electrons required for the RREA model as well as high energy bremsstrahlung photons that scatter away from the shower core and creating the shower front of the CREAS [Grieder 2010]. A diagram of a CREAS in the atmosphere is shown in Figure 1. The majority of secondary particles in the CREAS can be found in the shower front. Due to scattering, the particle density decreases with distance from the shower core.

Energetic secondary electrons lose energy via ionization and bremsstrahlung in the atmosphere, so they have a finite range before they stop and recombine with the atmospheric atoms and molecules. The range of electrons in air increases from tens of meters for 1 MeV electrons to over a kilometer for >1 GeV electrons at thunderstorm altitudes [Rakov and Uman 2003; NIST 2014] as shown in Figure 2. Without some method of gaining energy in the atmosphere, the majority of CREAS secondary electrons will range out shortly after being generated, so only the newest generation of secondary electrons exists at a given altitude in the atmosphere.

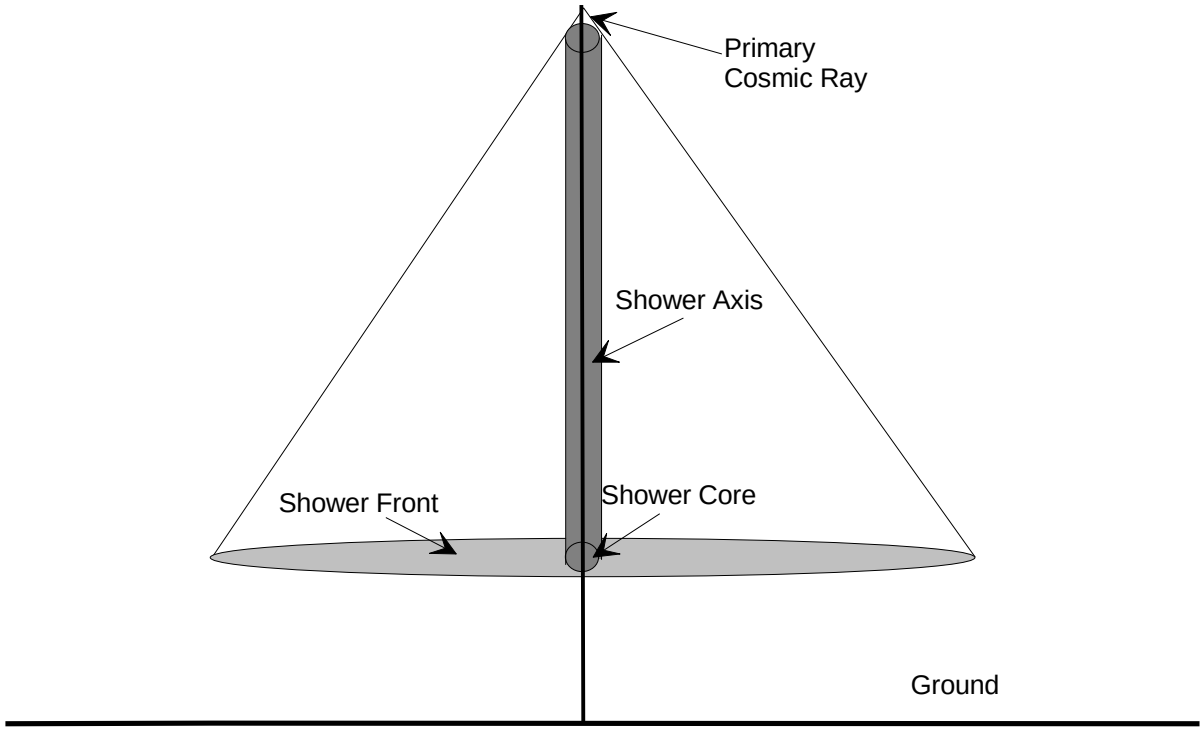


Figure 1: Diagram of a vertical CREAS developing in the atmosphere (not drawn to scale).

Thunderstorms produce strong electric fields that can affect high energy secondary electrons. Depending on the direction of the electric field, electrons are either accelerated or decelerated. Accelerated electrons have their range extended and are of higher energy than similar electrons in fair weather conditions, whereas decelerated electrons have their ranges reduced and are of lower energy than similar electrons in fair weather conditions. In very strong electric fields, high energy secondary electrons are accelerated sufficiently in the electric field to

more than compensate for the electrons' energy losses to ionization and bremsstrahlung. This causes the high energy electrons to have infinite range and become runaway electrons [Gurevich et al. 1992]. According to the RREA model, runaway electrons generate additional runaway secondary electrons through ionization in an exponential manner, in what is called an RREA. The runaway electrons in the RREA also generate a large number of low energy (~100 eV) secondary electrons through ionization, resulting in a low energy electron plasma. Conditions within this low energy electron plasma have been theorized to allow breakdown to occur in the atmosphere [Petersen et al. 2008; Milikh and Roussel-Dupre 2010].

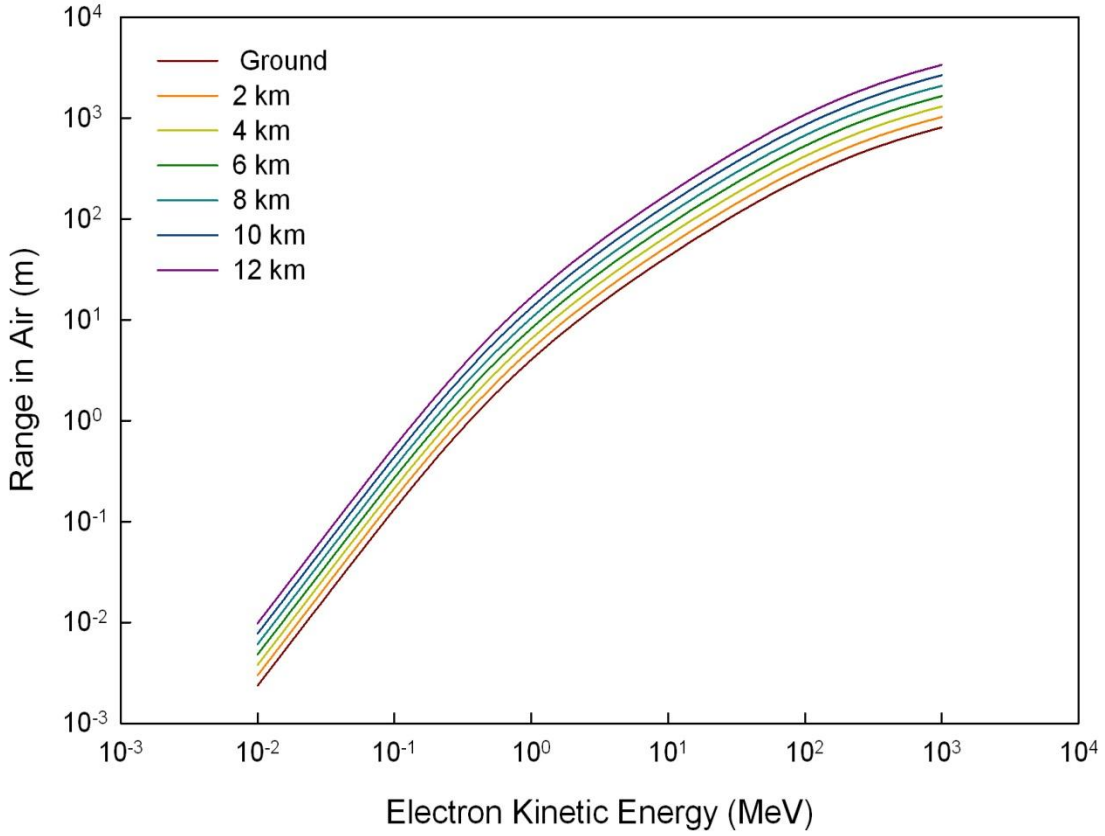


Figure 2: Range of electrons in air at various altitudes in fair weather conditions [NIST 2014].

## METHODS

### *Determining Fair Weather High Energy Electron Flux*

CREASs were simulated at different altitudes in the atmosphere with the cosmic ray Monte Carlo code CORSIKA (COsmic Ray SImulations for Kascade) 6.790 [Heck et al. 1998]. In order to properly simulate the propagation of CREAS secondary electrons in the atmosphere, the composition of the atmosphere and geomagnetic fields must be included in the simulation. The 1976 U.S. Standard Atmosphere [NOAA et al 1976; Heck et al. 1998] and geomagnetic field for Norman, OK [IGRF 2010] were used in this work.

Each CORSIKA simulation outputs the position relative to the shower core and energy of every secondary electron produced in a CREAS at a user determined observation altitude. For this work, only vertical CREASs were modelled, so that the distribution of CREAS secondary particles would be cylindrically symmetric around the shower axis. The area around the shower core was dividing into multiple rings at differential radial distances from the shower axis. The number and energy of secondary electrons were determined for each ring as,

$$n_e = n_e\ E_p, E_e, R, h\ , \tag{2}$$

where $n_e$ is the number of electrons with energy $E_e$ *and* a distance $R$ away from the shower axis in a CREAS at an altitude of $h$. For better statistics, multiple CREASs where simulated for each primary proton energy used and the data was combined to get an average $n_e$ for a given $E_p$. The number of simulations used for each of the initial CREAS energies is shown in Table 1. The amount of time per simulation increased linearly with primary energy, so the difference in the number of simulations for different initial CREAS energies are a compromise between statistics and amount of computer time [Heck et al. 2010].

Table 1: Number of CORSIKA 6.970 simulations for each initial CREAS energy.

| Initial CREAS Energy (eV) | Number of Simulations |
|---|---|
| $10^{10}$ | 10000 |
| $10^{11}$ | 10000 |
| $10^{12}$ | 10000 |
| $10^{13}$ | 1000 |
| $10^{14}$ | 1000 |
| $10^{15}$ | 100 |
| $10^{16}$ | 50 |

The secondary electron density, $\rho(E_p, E_e, R)$, can be found by

$$\rho\ E_p, E_e, R, h\ = \frac{n_e\ E_p, E_e, R, h}{A\ R}, \tag{3}$$

where $A(R)$ is the area of the ring where $n_e$ was found from equation (3). Figure 3 is a plot of the average secondary electron density as a function of distance from the shower core for the listed initial CREAS energies at 6 km altitude. From the secondary electron density, the secondary electron flux and energy spectrum can be determined for ambient conditions or for a single CREAS. The ambient secondary electron flux, $\varphi_{ambient}$, is made up of secondary electrons from all the CREASs that travel through a region of the atmosphere over a period of time:

$$\varphi_{ambient}\ h\ = \int_{0}^{R'} \int_{1\,MeV}^{E_e'} \int_{10^{10}eV}^{10^{16}eV} \varphi_{primary}\ E_p\ \ A\ R\ \rho\ E_p, E_e, R, h\ \ dE_p dE_e dR, \tag{4}$$

where $R'$ is the maximum distance a secondary electron is away from the shower core, and $E_e'$ is the maximum energy of a secondary electron. $R'$ = 10 km and $E_e'$ = $10^{11}$ eV (100 GeV) were used in this work due to $n_e < 1$ beyond those limits.

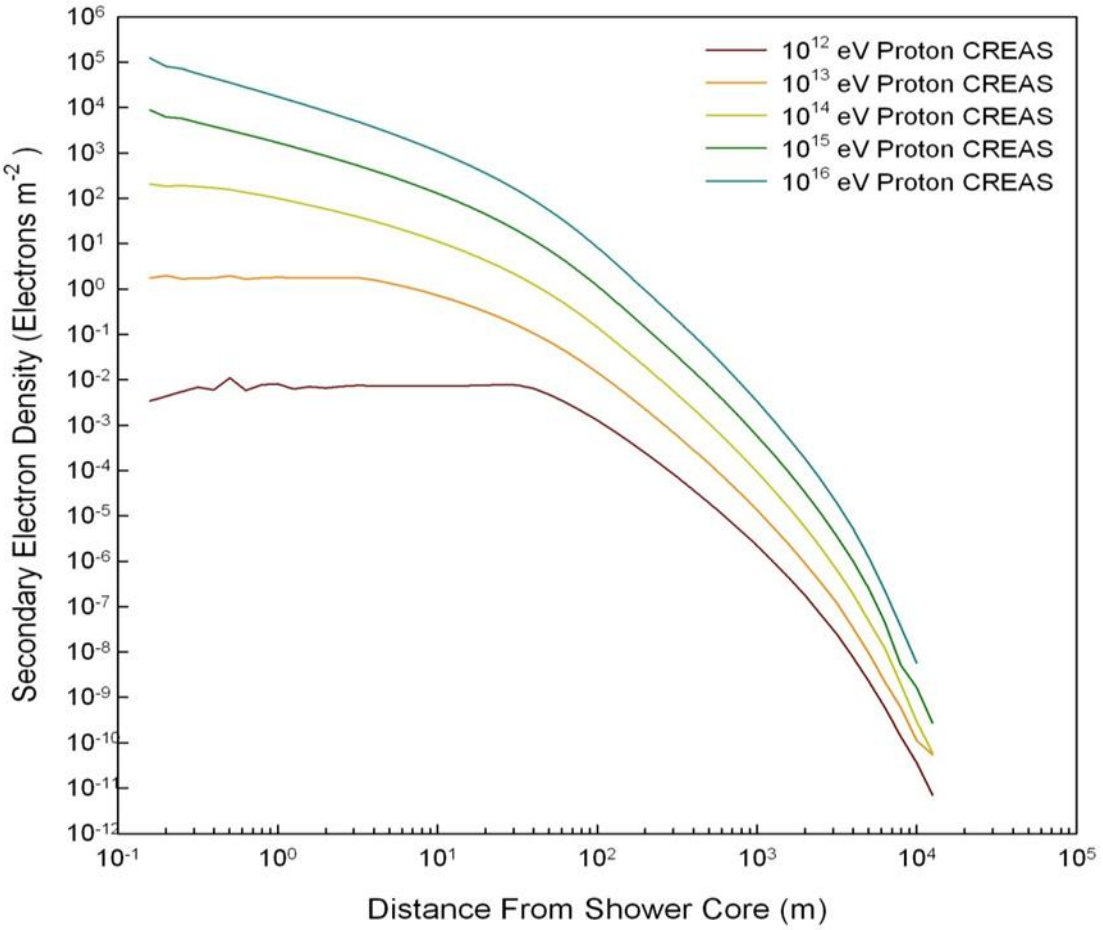


Figure 3: Secondary electron density from a vertical proton primary CREAS with listed initial energy as a function of distance from the shower core. The secondary electron density was calculated from CREAS simulations produced by CORSIKA.

The ambient secondary electron energy spectrum, $\phi_{ambient}$ is found by,

$$\phi_{ambient}\ E_e, h\ dE_e = \int_0^{R'} \int_{10^{10}eV}^{10^{16}eV} \varphi_{primary}\ E_p\ A\ R\ \rho\ E_p, E_e, R, h\ dE_p dR. \quad (5)$$

For the core of a CREAS, the secondary electron flux, $\varphi_{CREAS}$, is found by,

$$\varphi_{CREAS}\ E_p, h\ = \int_0^{R'} \int_{1\,MeV}^{E_e'} \rho\ E_p, E_e, R, h\ dE_e dR \quad (6)$$

and the secondary electron energy spectrum, $\phi_{CREAS}$, is found by,

$$\phi_{CREAS}\ E_p, E_e, h\ dE_e = \int_0^{R'} \rho\ E_p, E_e, R, h\ dR. \tag{7}$$

For the CREAs core flux and energy spectrum, *R'* = 10 m was used instead of 10 km for the ambient secondary electrons. Beyond 10 m from the shower axis, the secondary electron density energy spectrum changes from the shower core to shower front, so *R'* = 10 m was used instead of 10 km.

***Propagating Secondary Electrons Through a Thunderstorm***

Thunderstorms introduce two changes to the fair weather atmosphere that affect the development of CREAS: strong electric fields and increased water content in the air. CREAS secondary electrons are charged particles so they accelerate in an electric field. Electric fields associated with thunderstorms can be up to several hundred kilovolts per meter in magnitude [Marshall et al. 2005]. In electric fields >100 kV $m^{-1}$, high energy secondary electrons may start to run away in the electric field, producing a large increase in the number of high energy secondary electrons.

For electron <100 MeV, ionization collisions make up the dominat form of energy loss in the atmosphere [Grieder 2010]. The average amount of energy lost to ionization collisions by electrons of all energies is given by the Bethe-Bloche formula:

$$-\left(\frac{dE_e}{dx}\right)_{ion} = \left(\frac{e^2}{4\pi\varepsilon_0}\right)^2 \frac{2\pi N_0 z\rho}{mc^2\beta^2 A}\left[\ln\left(\frac{E_e\ E_e + mc^2\ \beta^2}{2I^2 mc^2}\right) + 1 - \beta^2 - \ln 2\left(2\sqrt{1-\beta^2} - 1 + \beta^2\right) + \frac{1}{8}\left(1 - \sqrt{1-\beta^2}\right)^2\right], \tag{8}$$

where *x* is the distance the electron travels through a material, *e* is the charge of an electron, $\varepsilon_0$ is the permittivity of free space, $N_0$ is Avogadro's number, *z* is the atomic number of the material, ρ is the density of the material, *m* is the mass of an electron, *c* is the speed of light, $\beta = v/c$, *v* is the velocity of the electron, *A* is the atomic mass of the material, and *I* is the mean ionization potential of the material [ICRU 1984]. The negative sign indicates that the electron is losing energy while traveling through a material.

The Bethe-Bloche formula determines the average amount of energy an electron loses to both soft and hard collisions. Soft collisions are glancing collisions between the high energy secondary electron and bound atomic electrons. As the high energy electron travels past the bound electron, a small amount of energy is transferred, which excites and possible ionizes the bound electron. A high energy electron typically loses ~40 eV in order to ionize one bound electron [ICRU 1979] even through the average ionization potentials for $N_2$ and $O_2$ are 15.6 and 12.2 eV, respectively [Bazelyan and Raizer 1998]. Soft collisions are responsible for high energy secondary electrons generating a low energy electron plasma. Hard collisions are direct collisions between high energy secondary electrons and bound electrons. In a hard collision, up to all of the high energy secondary electron's energy could be transferred to a bound electron. Hard collisions are how high energy secondary electrons generate additional high energy secondary electrons in the atmosphere. The average amount of energy lost to generate high energy secondary electrons can be determined from the Mott Scattering cross section:

$$\sigma\ E_e, W\ = \ \frac{e^2}{4\pi\varepsilon_o}\ ^2 \frac{2\pi N_o z\rho}{mc^2\beta^2 A} dR\ \ \frac{1}{E_e W^2} - \frac{1}{E_e W\ \ 1-W} \frac{mc^2\ \ 2E_e + mc^2}{E_e + mc^2\ \ ^2} + \frac{1}{E_e\ \ 1-W\ ^2} + \frac{T}{E_e + mc^2\ \ ^2} \tag{9}$$

where $\sigma$ is the Mott Scattering cross section, $W$ is ratio of the primary and secondary electron energies [Segre 1953]. It should be noted that the energy losses determined from Mott Scattering are already included in the Bethe-Bloche formula. This work assumed newly generated high energy secondary electrons have an average initial energy of 1 MeV.

For >100 MeV electrons, the dominat form of energy loss in the atmosphere is the production of bremsstrahlung photons. The average amount of energy lost to the production of bremsstrahlung photons is given by

$$-\ \frac{dE_e}{dx}\ _{brem} = \ \frac{e^2}{4\pi\varepsilon_0}\ ^2 \frac{\alpha z^2 N_0\ \ E_e + mc^2\ \rho}{m^2 c^4 A}\ 4ln\ \ \frac{2\ \ E_e + mc^2}{mc^2}\ \ - \frac{4}{3}\ , \tag{10}$$

where $\alpha$ is the fine structure constant [ICRU 1984]. Bremsstrahlung is a stochastic process where photons can be created with up to the kinetic energy of the electron, so to accurately determine the number and energy of the secondary photons, Monte Carlo simulation is required. However, the total kinetic energy lost by the electron to bremsstrahlung is accurately described by Equation (9). The total amount of energy lost by an electron while traveling through a material is given by,

$$\frac{dE_e}{dx}\ _{tot} = \ \frac{dE_e}{dx}\ _{ion} + \ \frac{dE_e}{dx}\ _{brem}. \tag{11}$$

Equation (11) is generally referred to as the stopping power in a material with equation (8) being the collisional stopping power and equation (10) is the radiative stopping power. In a compound material, such as air, the total stopping power is calculated from the stopping power for each of the materials that make up the compound:

$$\frac{dE_e}{dx}\ _{compound} \rho_{compound}^{-1} = \ _i\ \omega_i\ \ \frac{dE_e}{dx}\ _i \rho_i^{-1}, \tag{12}$$

where the index $i$ represents each of the materials that make up the compound and $\omega_i$ is the mass fraction of the $i$ th material within the compound [ICRU 1984]. In gaseous materials, the low energy bonds between molecules can be ignored when calculating stopping power [Ziegler et al 2008]. Within a thunderstorm, the air contains more water in various states than the U.S. Standard Atmosphere [NOAA et al. 1976; MacGorman et al. 2008], so the stopping power for electron inside a thunderstorm is slightly lower than in fair weather conditions [NIST 2014]. Table 2 shows the mean ionization potential $I$ and mass fractions for fair weather and thunderstorm conditions used in this work.

Table 2: Mean ionization potential $I$ and mass fractions $\omega_i$ for fair weather and thunderstorm conditions in the atmosphere [NOAA et al. 1976; ICRU 1984; MacGorman 2008].

| Element | $I$ (eV) | Fair Weather $\omega_i$ | Thunderstorm $\omega_i$ |
|---|---|---|---|
| H | 19.2 | 0.0000 | 0.0012 |
| N | 82.0 | 0.7617 | 0.7721 |
| O | 95.0 | 0.2262 | 0.2174 |
| Ar | 1880 | 0.0121 | 0.0093 |

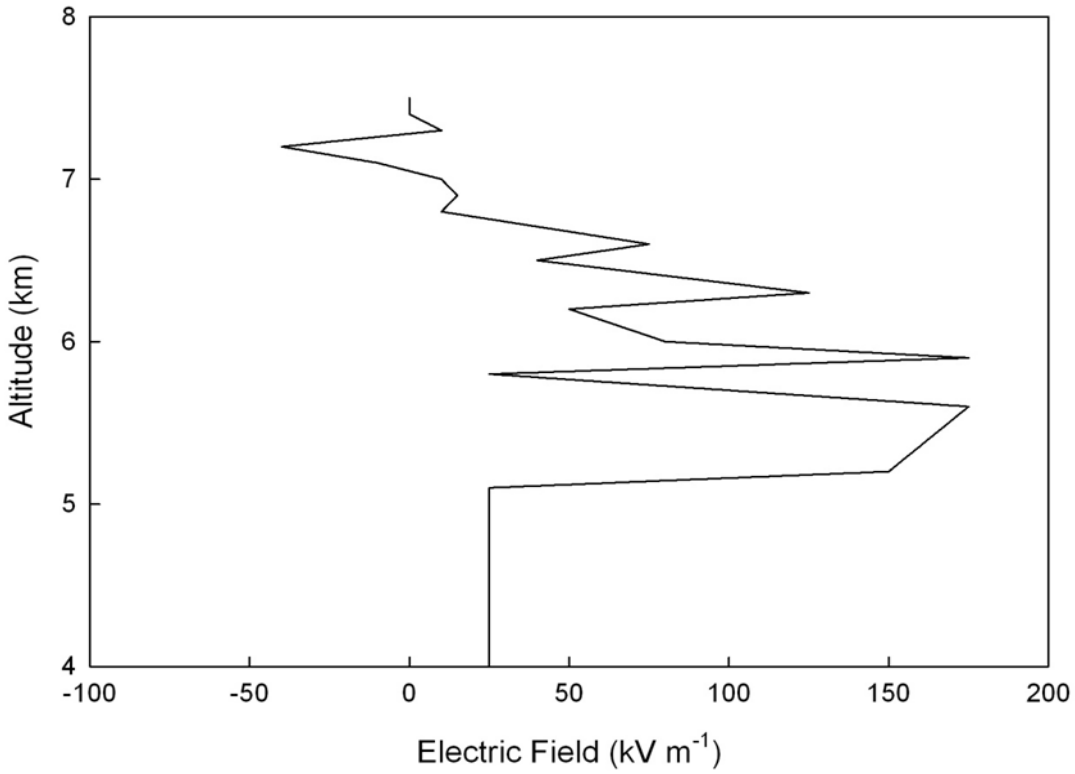


Figure 4: Parameterization of the vertical electric field measured in Marshall et al. [2005].

This work uses a parameterization of the vertical thunderstorm electric field measured by Marshall et al. [2005] shown in Figure 4. A positive electric field will accelerate electrons traveling in a downward moving CREAS. The thunderstorm electric field extends from 4 to 8 km altitude and varies between -50 and 175 kV $m^{-1}$. It reaches a maximum and stays relatively constant between 5 and 6 km altitudes. The change in energy of a CREAS secondary electron per distance due to the electric is given by:

$$\left(\frac{dE_e}{dx}\right)_{electron} h\ \Delta x = \left(\frac{dE_e}{dx}\right)_{compound} h\ \Delta x + e\varepsilon\ h\ \Delta x, \quad (13)$$

where $\varepsilon$ is thunderstorm's electric field at altitude $h$ for the traveled distance of $\Delta x$ . For this work, $\Delta x$ = 1 m.

## RESULTS

### *Fair Weather CREAS Secondary Electron Flux and Energy Spectrum*

The fair weather secondary electron flux for both ambient conditions, i.e. combination of all the secondary electrons from all the CREAS passing through a region in the atmosphere, and in the core of $10^{16}$ eV CREAS is shown in Figure 5. The fair weather flux is directly calculated from CORSIKA simulations by using equations (3) and (6). CREAS travel downwards through the atmosphere towards ground, so ambient secondary electron flux decreases exponentially with altitude from 12 km to the ground. The ambient secondary electron has a value of ~260 electrons $m^{-2}$ $sr^{-1}$ $s^{-1}$ at 8 km altitude. The exponential increase in the ambient secondary electron flux is due to the large number of low energy CREASs that develop high in the atmosphere and are attenuated at lower altitudes. In contrast, the secondary electron flux in the core of a $10^{16}$ eV CREAS first increases as it travels through the atmosphere until reaching a maximum in between 4 and 5 km before decreasing exponentially the rest of the way to the ground. High energy CREAS travel much farther through the atmosphere than low energy CREAS before reaching shower maximum, i.e. the largest amount of secondary particles [Grieder 2010]. CREAS produced by ~$10^{10}$ eV protons typically have their shower maximum >12 km altitudes, where the rarer $10^{16}$ eV CREAS have their shower maximum ~4 km altitude.

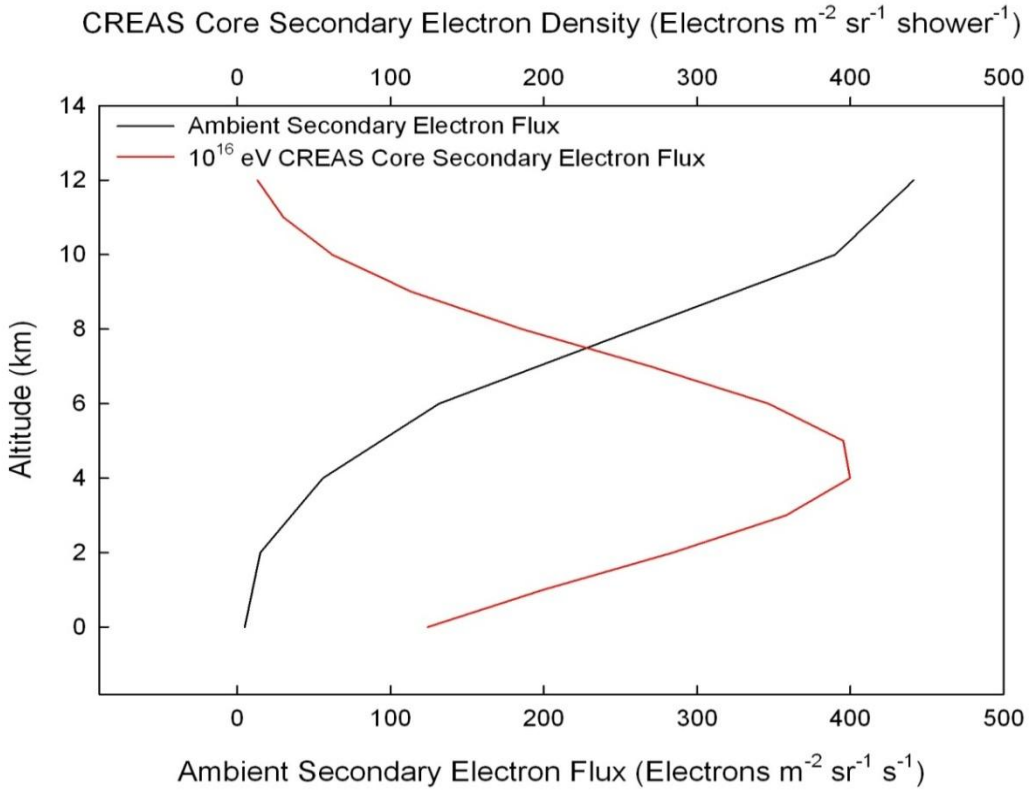


Figure 5: The fair weather CREAS secondary electron flux in ambient conditions and in the core of a $10^{16}$ eV CREAS. The fair weather CREAS secondary electron flux was calculated directly from CORSIKA simulations.

The ambient secondary electron energy spectrum is shown in Figure 6. The ambient secondary electron energy spectrum decreases with secondary electron energy. Due to the wide range of the secondary electron energies and differential fluxes, both scales are logarithmic and the ambient secondary electron energy spectrum can be approximated by a power law distribution.

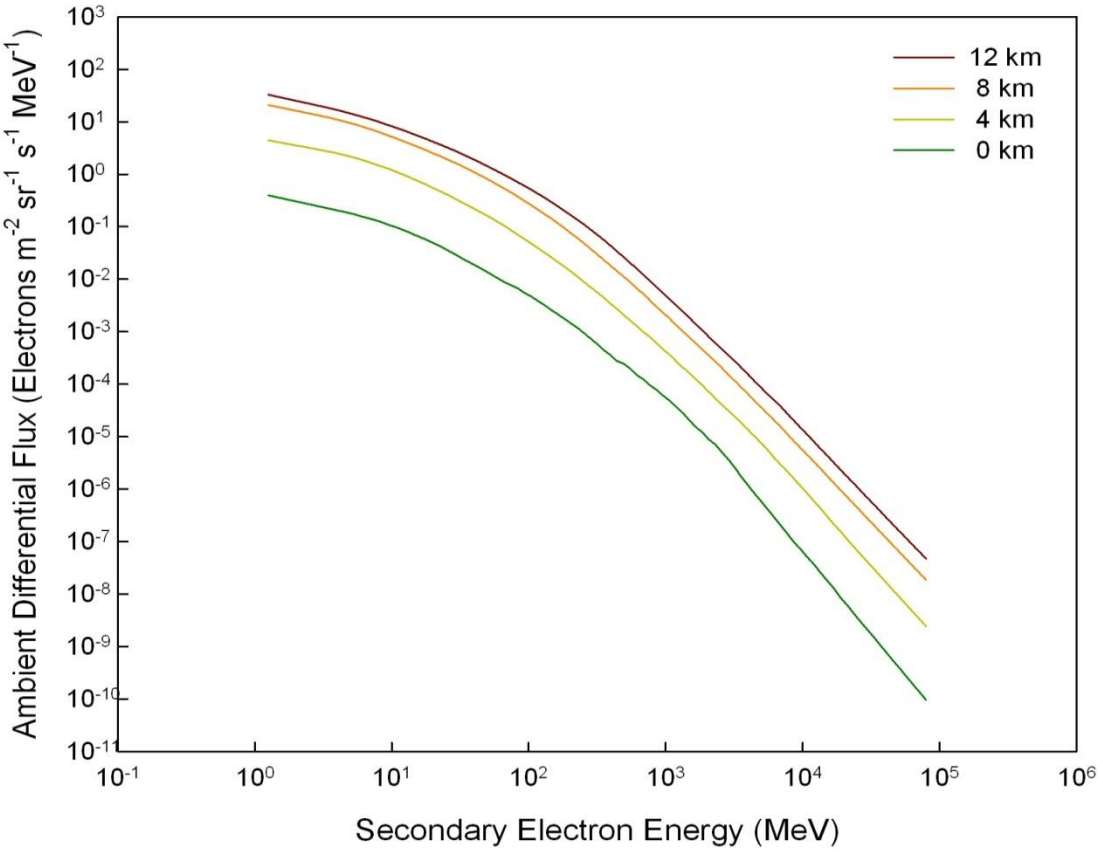


Figure 6: Fair weather ambient secondary electron energy spectrum at various altitudes. The fair weather ambient secondary electron energy spectrum was calculated directly from CORSIKA simulations.

The secondary electron energy spectrum inside the core of a $10^{16}$ eV CREAS is shown in Figure 7. The secondary electron energy spectrum inside a core of a CREAS decreases with secondary electron energy like the ambient secondary electron energy spectrum shown in Figure 6. However, there are less ~1 MeV and more >100 MeV secondary electrons within core of a $10^{16}$ eV CREAS that in ambient conditions. The reason these differences is due to lower energy secondary electrons having a higher probability of scattering out of CREAS shower cores and becoming part of the shower front than higher energy secondary electrons. In ambient conditions, the most of the secondary electrons are part of the shower front of one of the multiple CREASs traveling through that region of the atmosphere and so are typically of lower energy. On the contrary, the highest energy secondary electrons are located in the core of high energy CREAS along with the fraction of the lower energy secondary electrons that do not scatter out of the shower core.

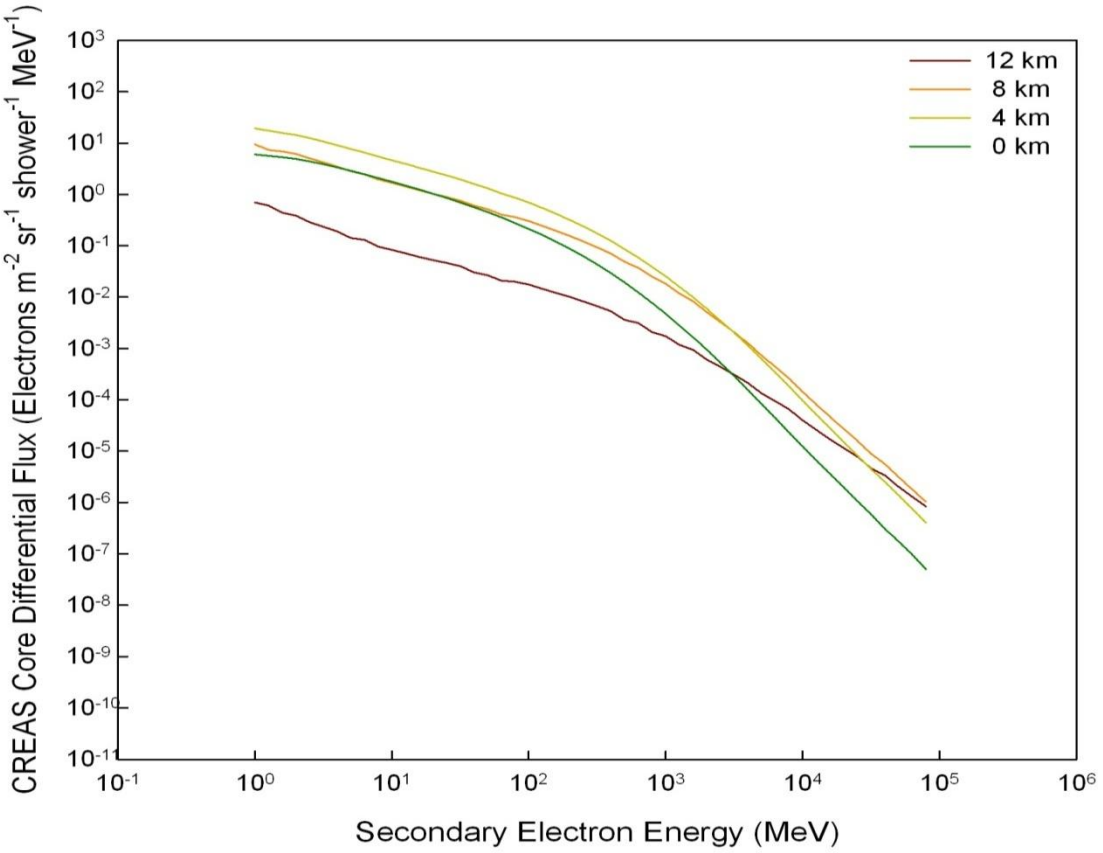


Figure 7: Fair weather secondary electron energy spectrum inside the core of a $10^{16}$ eV CREAS at various altitudes. The secondary electron energy spectrum was calculated directly from CORSIKA simulations.

***Thunderstorm CREAS Secondary Electron Flux and Energy Spectrum***

Figure 8 displays the ambient secondary electron flux in a thunderstorm that was generated by the electric field profile shown in Figure 4. Also shown in Figure 8 is the fair weather ambient secondary electron flux. The electric field was not measured above 8 km, so fair weather conditions are assumed between 8 and 12 km altitude where the CREAS enter the thunderstorm. Due to the presence of the electric field, the change in energy and the number of high energy secondary must be calculated using equations (9) and (12) starting with the fair weather secondary electron energy spectrum determined from CORSIKA simulations at 8 km. As the CREASs travel through the thunderstorm, the electric field increases in strength from 8 km to 6 km and the ambient secondary electron flux increases relative to the fair weather ambient secondary electron flux. By 6 km altitude, the ambient secondary electron flux had increased an order of magnitude relative to the fair weather ambient secondary electron flux. Between 5 and 6 km, the electric field reaches and maintains its maximum strength. Within this maximum electric field region, the ambient secondary electron flux increases another order of magnitude relative to the fair weather ambient secondary electron flux. Below 5 km altitude, the electric field decreases rapidly to 25 kV $m^{-1}$. The ambient secondary electron flux also quickly

decreases in this region and reaches a value slightly larger than the fair weather secondary electron flux.

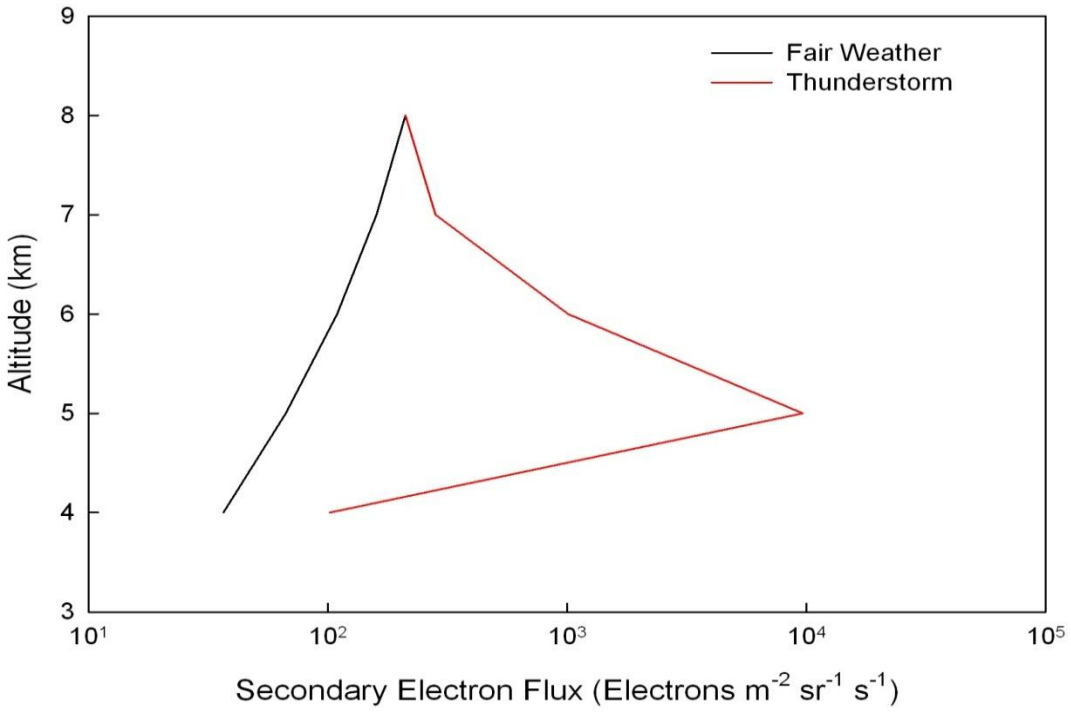


Figure 8: Ambient secondary electron flux in fair weather and thunderstorm conditions.

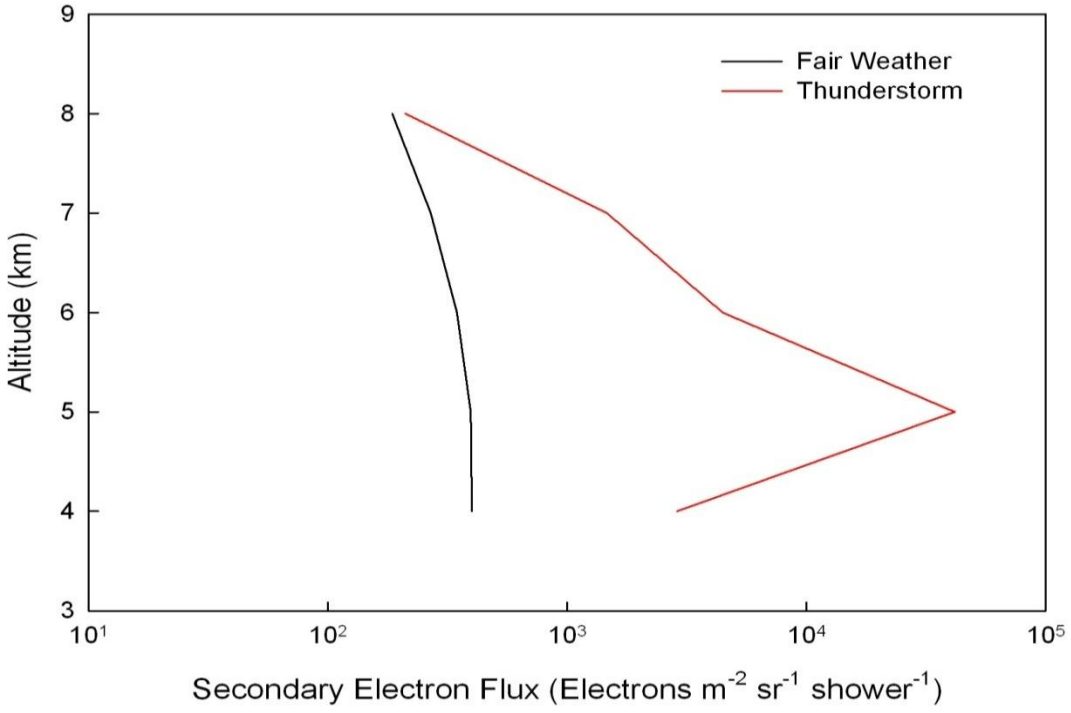

Figure 9: Secondary electron flux in fair weather and thunderstorm conditions inside the core of a $10^{16}$ eV CREAS.

Figure 9 shows the secondary electron energy flux in both fair weather and thunderstorm conditions inside the core of a $10^{16}$ eV CREAS. Like the ambient secondary electron energy spectrum, the secondary electron energy flux inside the core of a $10^{16}$ eV CREAS is calculated from the fair weather secondary electron flux determined from the CORSIKA simulations at 8 km altitude and propagated through the thunderstorm using equations (9) and (12). The secondary electron flux inside the core of a $10^{16}$ eV CREAS core increases relative to the fair weather secondary electron flux as the electric field increases in strength as the CREAS travels from 8 to 6 km altitude. In the region of maximum electric field strength, the secondary electron flux increases two orders of magnitude relative to the fair weather secondary electron flux as the CREAS travels from 6 km to 5 km altitude. In the weak electric field region between 4 and 5 km, the secondary electron flux decreases back towards the fair weather secondary electron flux value.

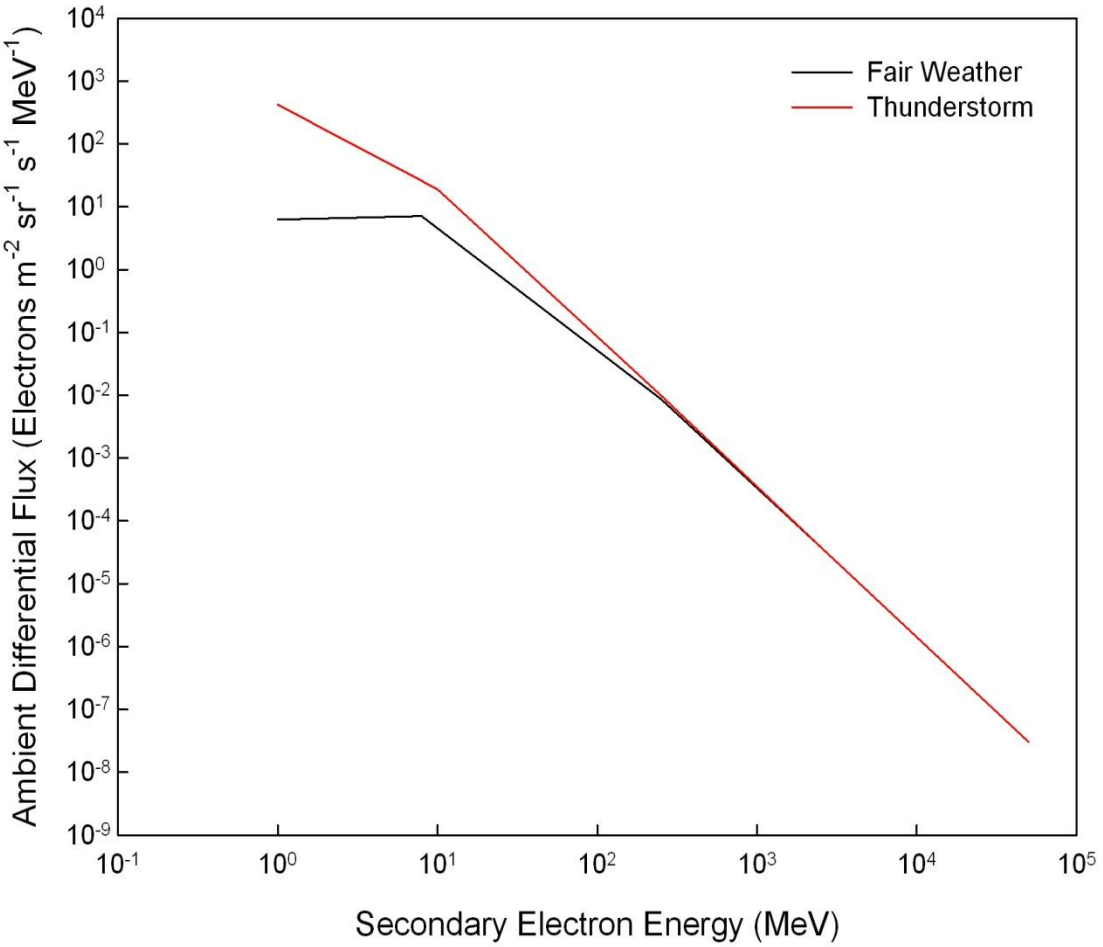


Figure 10: Ambient differential secondary electron flux in fair weather and thunderstorm conditions at 5 km altitude.

The greatest enhancement of the secondary electron flux occurs between 5 and 6 km altitude where the electric field is at a maximum. This region of maximum electric field strength is also where RREA theory predicts that lightning should occur. Figures 10 and 11 show the secondary electron energy spectrum in ambient conditions and the core of a $10^{16}$ eV CREAS, respectively, at 5 km altitude where the secondary electron flux is greatest. In Figures 10 and 11, the number of ~1 MeV electrons increases by two orders of magnitude in thunderstorm conditions relative to fair weather conditions. As the secondary electron energy increases, thunderstorm enhancement in the number of electrons relative to the fair weather conditions decreases till energies of ~1 GeV. This enhancement in the number of secondary electrons of a given energy relative to fair weather conditions is due to the secondary electrons accelerating and running away in the strong electric field. One MeV electrons runaway in the strong electric fields found between 5 and 6 km altitude and no longer range out over that distance. For >100 MeV secondary electrons, the electric field decreases the overall amount of energy loss to traveling through the atmosphere, so the secondary electrons retain their high energy for a much longer distance. By retaining their energy longer, the >100 MeV secondary electrons generate more high energy secondary electrons through hard collisions and high energy (>1 MeV) bremsstrahlung photons than would be generated in fair weather conditions [Rossi 1952].

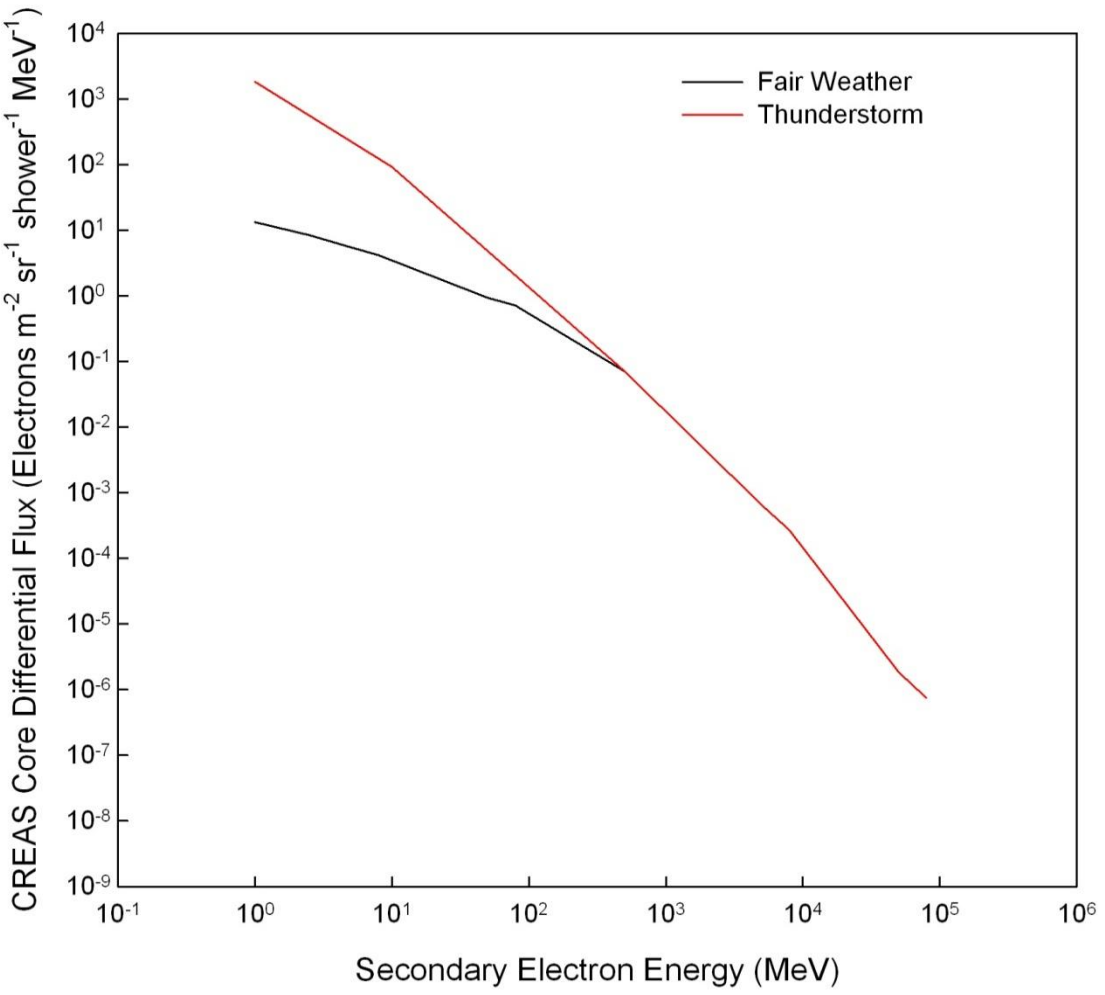

Figure 11: Secondary electron energy spectrum in the core of a $10^{16}$ eV CREAS in fair weather and thunderstorm conditions at 5 km altitude.

## CONCLUSIONS

The RREA model proposes that the number of high energy secondary electrons increases exponentially in the strong electric field region of a thunderstorm. Eventually, the high energy secondary electrons become dense enough to breakdown the atmosphere and initiate a lightning discharge. Using simulated high energy secondary electron distributions from the cosmic ray Monte Carlo code CORSIKA 6.790 and a parameterization of the electric field measured in Marshall et al. [2005], we show that the secondary electron flux increases by two orders of magnitude within the strong electric field region of the thunderstorm compared to fair weather secondary electron flux. From our calculated secondary electron energy spectrum, the strong electric fields increased the number of high energy secondary electrons all the way up to ~1 GeV. The enhancement of the >100 MeV secondary electrons increases the production of >1 MeV secondary electron and bremsstrahlung photons. Studies of the RREA model [Gurevich et al. 1992; Carlson et al. 2008] have focused on the effects run away acceleration has on the <10 MeV secondary electron population, while this work shows electron run away affects even >100 MeV secondary electrons. The enhancement in the >100 MeV secondary electron flux and associated bremsstrahlung production may be responsible for the Thunderstorm Ground Enhancements (TGE) measured in Chilingarian et al. [2012].

A two order of magnitude enhancement of the high energy secondary electron flux inside the core of a $10^{16}$ eV CREAS is not enough to generate the electron density required for streamer formation [Dawson and Winn 1965]. However, high energy secondary electrons also generate a large number of low energy secondary electrons through soft collisions. These low energy secondary electrons stay behind the passing CREAS shower front and are dense enough to form a plasma in the atmosphere. This plasma has been theorized to be required in lightning initiation [Petersen et al. 2008, Milikh and Roussel-Dupre 2010]. More work is needed done to determine the necessary high energy secondary electron flux that can generate a sufficiently dense enough low energy electron plasma to initiate a lightning discharge.

## ACKNOWLEDGMENTS

This research was funded through the DARPA Nimbus program.

## REFERENCES

Bazelyan, E. M. and Yu. P. Raizer, 1998: *Spark Discharge*. CRC Press, Boca Raton, Florida, USA, 294pp.

Carlson, B. E., N. G. Lehtinen, and U. S. Inan, 2008: Runaway relativistic electron avalanche seeding in the Earth's atmosphere. *J. Geophys. Res.*, **113**, A10307.

Chilingarian, A., B. Mailyan, and L. Vanyan, 2012: Recovering of the energy spectra of electrons and gamma rays coming from the thunderclouds. *Atmos. Res.*, **114-115**, 1-16.

Dawson, G. A. and W. P. Winn, 1965: A model for streamer propagation. Zeitschrift ftir Physik, **183**, 159-171.

Dorman, Lev I., 2004: *Cosmic Rays in the Earth's Atmosphere and Underground*. Kluwer Academic Publishers, Dordrecht, Netherlands, 855pp.

Dwyer, J. R., M. A. Uman, H. K. Rassoul, M. Al-Dayeh, L. Caraway, J. Jerauld, V. A. Rakov, D. M. Jordan, K. J. Rambo, V. Corbin, B. Wright, 2003: Energetic Radiation Produced During Rocket-Triggered Lightning. *Science*, **299**, 694-697.

Gurevich, A. V., G. M. Milikh, and R. Roussel-Dupre, 1992: Runaway electron mechanism of air breakdown and preconditioning during a thunderstorm. *Phys. Lett. A*, **165**, 463-468.

Gurevich, A. V., Y.V. Medvedev, and K.P. Zybin, 2004: Thermal electrons and electric current generated by runaway breakdown effect. *Phys. Lett. A*, **321**, 179-184.

Grieder, Peter K. F., 2010: Extensive Air Showers: High Energy Phenomena and Astrophysical Aspects-A Tutorial, Reference Manual and Data Book. Springer, Heidelberg, Germany, 1113pp.

Heck, D., J. Knapp, J. N. Capdevielle, G. Schatz and T. Thouw, 1998: Report FZKA 6019. Forschungszentrum Karlsruhe, <https://web.ikp.kit.edu/corsika/physics_description/corsika_phys.html>, 90pp.

Heck, D., T. Pierog, G. Poghosyan, and R. Engel, 2010: Challenges of simulating air showers at ultra-high energy. Proceedings of the Computational Methods in Science and Engineering (SimLabs@KIT 2010), Karlsruhe, Nov. 29-30, 2010, 87-90.

Horandel, J. R., 2003: On the knee in the energy spectrum of cosmic rays. *Astropart. Phys.*, **19**, 193-220.

International Association of Geomagnetism and Aeronomy (IAGA), Working Group V-MOD, 2010: International Geomagnetic Reference Field: the eleventh generation. *Geophy. J. Int.*, **183**, 1216-1230.

International Commission on Radiation Units and Measurements (ICRU), 1979: Average Energy Required to Produce an Ion Pair. ICRU Report 31, 52pp.

International Commission on Radiation Units and Measurements (ICRU), 1984: Stopping Powers for Electrons and Positrons. ICRU Report 37, 271pp.

MacGorman D.R., W. D. Rust, T. J. Schuur, M. I. Biggerstaff, J. M. Straka, C. L. Ziegler, E R. Mansell, E. C. Bruning, K. M. Kuhlman, N. R. Lund, N. S. Biermann, C. Payne, L. D. Carey, P. R. Krehbiel, W. Rison, K. B. Eack, and W. H. Beasley, 2008: TELEX The Thunderstorm Electrification and Lightning Experiment. *Bull. Amer. Meteor. Soc.*,**89**, 997-1013.

Marshall, T. C., M. Stolzenburg, C. R. Maggio, L. M. Coleman, P. R. Krehbiel, T. Hamlin, R. J. Thomas, and W. Rison, 2005: Observed electric fields associated with lightning initiation. *Geophys. Res. Lett.*, **32**, L03813.

McCarthy M. P. and G. K. Parks, 1992: On the modulation of X ray fluxes in thunderstorms. *J. Geophys. Res.*, **97**, 5857–5864.

Milikh G. and R. Roussel-Dupre, 2010: Runaway breakdown and electrical discharges in thunderstorms. *J. Geophys. Res.*, **115**, A00E60.

National Institute of Standards and Technology (NIST), 2014: ESTAR: Stopping Power and Range Tables for Electrons. <http://physics.nist.gov/PhysRefData/Star/Text/ESTAR.html>

National Oceanic and Atmospheric Administration (NOAA), National Aeronautics and Space Administration (NASA), and United States Air Force, 1976: *U.S. Standard Atmosphere, 1976*. U.S. Government Printing Office, Washington D.C., USA.

Petersen, D., M. Bailey, W. H. Beasley, and J. Hallett, 2008: A brief review of the problem of lightning initiation and a hypothesis of initial lightning leader formation. *J. Geophys. Res,* **113**, D17205.

Rakov, Vladimir A. and Martin A. Uman, 2003: *Lightning: Physics and Effects*. Cambride University Press, Cambridge, UK, 687pp.

Rossi, B., 1952: High-Energy Particles. Prentice-Hall, Inc., Englewood Cliffs, NJ, USA, 569pp.

Segre E., editor., 1953: *Experimental Nuclear Physics*, Vol 1, John Wiley and Sons, Inc. New York, 789pp.

Ziegler J. F., J. P. Biersack, and M. D. Ziegler, 2008: *SRIM: The Stopping and Range of Ions in Matter*. SRIM Co., 400pp.